EUROPEAN SOCIETY OF RADIOLOGY
European Radiology

BREAST

Discrimination between HER2-overexpressing, -low-expressing, and -zero-expressing statuses in breast cancer using multiparametric MRI-based radiomics

Shaoyan Zheng[1,2†], Zehong Yang[2,3†], Guangzhou Du[1], Yiwei Zhang[1], Chuling Jiang[1], Tingting Xu[1], Bingli Li[1], Danfeng Wang[1], Ya Qiu[2,3], Daiying Lin[1*], Xiang Zhang[2,3*] and Jun Shen[2,3]

Abstract

Objectives To explore the performance of multiparametric MRI-based radiomics in discriminating different human epidermal growth factor receptor 2 (HER2) expressing statuses (i.e., HER2-overexpressing, HER2-low-expressing, and HER2-zero-expressing) in breast cancer.

Methods A total of 771 breast cancer patients from two institutions were retrospectively studied. Five-hundred-eighty-one patients from Institution I were divided into a training dataset ($n_1 = 407$) and an independent validation dataset ($n_1 = 174$); 190 patients from Institution II formed the external validation dataset. All patients were categorized into HER2-overexpressing, HER2-low-expressing, and HER2-zero-expressing groups based on pathologic examination. Multiparametric (including T2-weighted imaging with fat suppression [T2WI-FS], diffusion-weighted imaging [DWI], apparent diffusion coefficient [ADC], and dynamic contrast-enhanced [DCE]) MRI-based radiomics features were extracted and then selected from the training dataset using the least absolute shrinkage and selection operator (LASSO) regression. Three predictive models to discriminate HER2-overexpressing *vs.* others, HER2-low expressing *vs.* others, and HER2-zero-expressing *vs.* others were developed based on the selected features. The model performance was evaluated using the area under the receiver operating characteristic curve (AUC).

Results Eleven radiomics features from DWI, ADC, and DCE; one radiomics feature from DWI; and 17 radiomics features from DWI, ADC, and DCE were selected to build three predictive models, respectively. In training, independent validation, and external validation datasets, radiomics models achieved AUCs of 0.809, 0.737, and 0.725 in differentiating HER2-overexpressing from others; 0.779, 0.778, and 0.782 in differentiating HER2-low-expressing from others; and 0.889, 0.867, and 0.813 in differentiating HER2-zero-expressing from others, respectively.

Conclusions Multiparametric MRI-based radiomics model may preoperatively predict HER2 statuses in breast cancer patients.

---

† Shaoyan Zheng and Zehong Yang contributed equally to this work.

*Correspondence:
Daiying Lin
lindaiying917@163.com
Xiang Zhang
zhangx345@mail.sysu.edu.cn
Full list of author information is available at the end of the article

Springer

Zheng *et al. European Radiology* (2024) 34:6132–6144

6133

Clinical relevance statement The MRI-based radiomics models could be used to noninvasively identify the new three-classification of HER2 expressing status in breast cancer, which is helpful to the decision-making for HER2-target therapies.

Key Points

• *Detecting HER2-overexpressing, HER2-low-expressing, and HER2-zero-expressing status in breast cancer patients is crucial for determining candidates for anti-HER2 therapy.*

• *Radiomics features from multiparametric MRI significantly differed among HER2-overexpressing, HER2-low expressing, and HER2-zero-expressing breast cancers.*

• *Multiparametric MRI-based radiomics could preoperatively evaluate three different HER2-expressing statuses and help to determine potential candidates for anti-HER2 therapy in breast cancer patients.*

Keywords Neoplasms (breast), Multiparametric magnetic resonance imaging, ERBB2 protein (human)

Introduction

Breast cancer is the leading type of cancer and a primary contributor to cancer-associated mortality among the female population [1]. Human epidermal growth factor receptor 2 (HER2) is a prototypic oncogene of breast cancer. It plays a crucial role in prognostic evaluation and is an established therapeutic target with high response rates [2]. Traditionally, based on immunohistochemistry (IHC) and in situ hybridization (ISH), breast cancer is dichotomously classified as HER2-overexpressing status (IHC score 3+ or IHC 2+ with ISH amplification) and HER2-negative status (IHC score 0 or 1+, or IHC 2+ without ISH amplification) to select patients for HER2-targeted therapy [3]. However, in a recently proposed classification system, HER2-negative cases in traditional classifying criteria are sub-classified as HER2-low-expressing status (IHC 1+ or IHC 2+ without ISH amplification) and HER2-zero-expressing status (IHC score 0) [3, 4]. HER2-low-expressing, accounting for more than half of all traditionally HER2-negative breast cancers, have different biological characteristics and clinical outcomes compared with HER2-zero-expressing breast cancers or HER2-overexpressing breast cancers [2, 3, 5, 6]. Patients with HER2-zero-expressing breast cancers might be excluded from anti-HER2 therapy, and patients with HER2-overexpressing could benefit from traditional HER2-targeted therapy such as trastuzumab [3]. With the emergence of innovative HER2-targeted modalities like antibody–drug conjugates, even individuals exhibiting lower levels of HER2 expression might potentially derive therapeutic advantages from this medicinal intervention [4, 5, 7, 8]. Thus, identifying HER2-overexpressing, HER2-low-expressing, and HER2-zero-expressing statuses in patients with breast cancer could be highly desirable for determining potential candidates for anti-HER2 therapy [9].

Preoperative HER2 status assessment is usually based on pathologic analysis of biopsy specimens. However, breast cancer has considerable heterogeneity at multiple levels, affecting clinical behavior and therapeutic response [6]. The limited biopsy tissue may not comprehensively represent the entire tumor's genetic, epigenetic, and phenotypic alterations [10, 11]. In addition, genetic profiling based on pretreatment biopsy is performed at a single time point, but tumor biology potentially changes over time and during or after treatment [7]. Furthermore, the percutaneous breast tumor biopsy is an invasive procedure. Therefore, a simple, practical, and noninvasive method is needed to assess the HER2-expressing status before treatment in breast cancer patients.

MRI is widely used for breast tumor detection, categorization, and monitoring neoadjuvant treatment effects [12]. Radiomics analysis of MR images can translate medical images into high-dimensional data, reflecting the tumoral molecular properties and tumoral heterogeneity in the subtle and spatial view [13]. Several MRI-based radiomics models, including single-parametric and multiparametric MRI, have been proposed to predict traditionally classified HER2-overexpressing and HER-negative status [13, 14]. Recently, two studies have applied MRI-based radiomics models to distinguish HER2-zero, -low, and -overexpressing statues of breast cancer [15, 16]. Ramtohul et al developed an MRI radiomics signature to discriminate the HER2-low and -positive *vs.* HER2-zero cancers [15]. The HER2-positive *vs.* HER2-low cancers could be further distinguished by a model incorporating the pathologic characteristic (histologic type) based on the pretreatment biopsy and MRI findings (presence of nonmass enhancement, multiple or single lesions) [15]. Bian et al found that the radiomics models based on the intratumoral and peritumoral radiomic features from multiparametric MRI could distinguish HER2-positive *vs.* HER2-negative breast cancers and HER2-low *vs.* HER2-negative cancers [16]. These results indicate that the three classified HER2 statuses of breast cancer may have distinct microstructure

6134

Zheng *et al. European Radiology* (2024) 34:6132–6144

characteristics, which can be captured and discriminated by MRI-based radiomics features.

In this study, based on breast cancer data from two institutions, we developed and validated three multiparametric MRI-based radiomics predictive models for noninvasively discriminating the HER2-overexpressing *vs.* others, HER2-low-expressing *vs.* others, and HER2-zero-expressing *vs.* others status. Our study aims to predict HER2 status preoperatively through MRI-based radiomics, aiding in selecting candidates for traditional/new HER2-targeted therapies and identifying those who can be exempted from anti-HER2 treatment.

Methods

Ethics

This retrospective investigation obtained approval from the Ethics Committees of the respective institutions, with informed consent waived due to the study's retrospective design.

Study population

From January 2016 to July 2022, 651 breast cancer patients from Shantou Center Hospital (hereafter, Institution I) were collected; between January 2019 and September 2020, 275 breast cancer patients from Sun Yat-Sen Memorial Hospital, Sun Yat-Sen University (hereafter, Institution II), were collected. The patient enrollment pathway is presented in Fig. 1. The inclusion criteria comprised the following: (1) female individuals diagnosed with primary breast cancer through pathological examination; (2) patients who underwent breast multiparametric MRI; (3) HER2 status was determined by the IHC and/or ISH of postsurgical specimens. The exclusion criteria were as follows: (1) pathologic results of HER2 expressing status were incomplete or not available; (2) incomplete MRI data or poor quality of MRI images such as motion artifacts; (3) patients underwent breast MRI after breast lesion biopsy, surgery, or neoadjuvant therapy; (4) patients underwent neoadjuvant therapy before breast surgery and pathologic examination. The tumor size was not an inclusion or exclusion criterion in this study.

Clinicopathologic characteristics of patients

The clinical characteristics, including the patient's age and family history of breast cancer, were obtained from the electronic medical record system. The pathologic characteristics of breast cancer, including histology (invasive ductal carcinoma or others), HER2 status, hormone receptor (estrogen receptor [ER] and progesterone receptor [PR]) status, and Ki-67 index were collected from the hospital's pathology system. ER or PR negativity was defined as less than 1% of tumor cells showing positive nuclear staining, while ER or PR positivity was defined as 1% or more of tumor cells exhibiting positive nuclear staining. The threshold for Ki-67 was set at less than 14% for low Ki-67 level and 14% or more for high Ki-67 level.

HER2 status classification

HER2 status was determined through IHC or ISH, following the clinical practice guidelines for HER2 testing in breast cancer issued by the American Society of Clinical Oncology/College of American Pathologists [4, 17]. Further ISH testing was done for IHC 2+ results. Patients were grouped into HER2-overexpressing (IHC 3+ or IHC 2+ with ISH amplification), HER2-low-expressing (IHC 1+ or IHC 2+ without ISH amplification), and HER2-zero expressing (IHC 0) [3, 14].

MRI acquisition

MRI was conducted using a 3.0-T MRI scanner (Siemens Magnetom Verio) or 1.5-T MRI scanner (Siemens Magnetom Area) with an 8-channel breast coil in Institution I, and 1.5 T MR scanner (Siemens Magnetom Avanto) with an 8-channel breast coil in Institution II. Imaging sequences included axial T1-weighted imaging (T1WI), axial turbo-spin-echo T2-weighted imaging (T2WI) with fat suppression (FS), axial single-shot diffusion-weighted imaging (DWI), and axial dynamic contrast-enhanced (DCE) imaging. The apparent diffusion coefficient (ADC) map was calculated in a pixel-by-pixel manner from DWI via the manufacturer's software (syngo.via; Siemens Healthcare), based on the formula $ADC = -In[S(b_2) - S(b_1)] \div (b_2 - b_1)$, where $S(b_1)$ and $S(b_2)$ were the signal intensity corresponding to *b* values of 50 and 800 s/mm^2 at Institution I, and 0 and 800 s/mm^2 at Institution II, respectively. Before DCE, an initial T1WI-FS pre-contrast scan was performed, followed by intravenous gadolinium contrast injection (Gadopentetate Dimeglumine, Magenvist, 0.2 mmol/kg at 2 mL/s in Institution I; Gd-DTPA-BMA, Omniscan, 0.1 mmol/kg at 3.5 mL/s in Institution II), with 20 mL saline flush. DCE consisted of one pre-contrast and five post-contrast phases with each phase for 60 s at Institution I, and two pre-contrast and 38 post-contrast phases with 8-s temporal resolution at Institution II. MRI sequence details are given in Table 1.

Two radiologists (reader 1: Y.W.Z., 13 years of breast lesion expertise from Institution I; reader 2: Y.Q., 7 years of breast lesion experience from Institution II) measured the long tumor diameter on the peak-enhanced DCE phase (2nd phase in Institution I, 12th in Institution II) [18] on ITK-SNAP software (version 3.8.0, http://www.itksnap.org). The average value of each breast tumor was recorded.

Data of breast cancer patients from institution I between Jan 2016 and July 2022 (n_1= 651) and institution II between Jan 2019 and September 2020 (n_2=275)

Excluded for the following reasons (n_1=70, n_2=85):
   --Pathologic results incompplete or not available (n_1=22, n_2=15)
   --Incomplete MRI data or poor quality of MR images (n_1=12, n_2=10)
   --Received biopsy, surgery or neoadjuvant therapy before MRI (n_1=16, n_2=30)
   --Underwent neoadjuvant therapy before breast surgery and pathologic examination(n_1=20, n_2=30)

Patients in this retrospective study (n_1=581, n_2=190)

Training dataset (n_1=407)

Independent validation dataset (n_1=174)

External validation dataset (n_2=190)

HER2-overexpressing *vs.* others (n_1=128)

HER2-low-expressing *vs.* others (n_1=201)

HER2-zero-expressing *vs.* others (n_1=78)

HER2-overexpressing *vs.* others (n_1=64)

HER2-low-expressing *vs.* others (n_1=72)

HER2-zero-expressing *vs.* others (n_1=38)

HER2-overexpressing *vs.* others (n_1=64)

HER2-low-expressing *vs.* others (n_1=87)

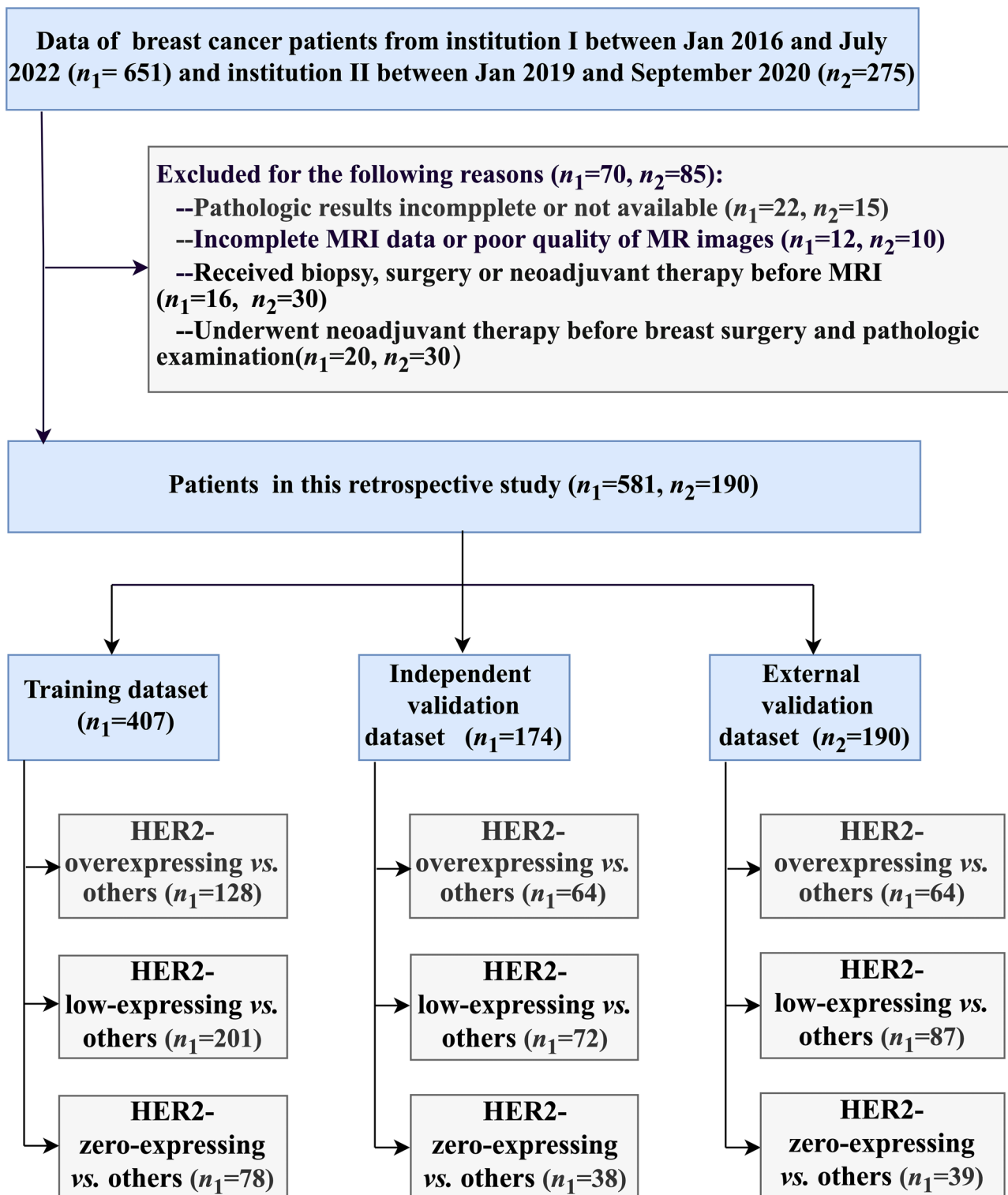HER2-zero-expressing *vs.* others (n_1=39)

Fig. 1 The patient enrollment pathway in two institutions. n_1, number of patients in institution I; n_2, number of patients in institution II

6136

Zheng *et al. European Radiology* (2024) 34:6132–6144

Table 1 Multiparametric breast MRI sequences in two institutions

Sequence	Institution	TE (ms)	Fat suppression	FOV (mm)	Matrix	Parallel imaging factor	Slice thickness (mm)	b value (s/mm²)	Acquisition time
T1WI	I	2.46	No	340×340	448×448	2	1.3	–	1 min 2 s
	II	2.39	Yes	350×350	384×384	2	4	–	2 min 20 s
T2WI	I	61	Yes	340×340	320×320	2	4	–	3 min 37 s
	II	107	Yes	350×350	320×224	2	4	–	2 min 46 s
DWI	I	68	Yes	360×360	68×144	2	4	50, 400, 800	3 min 3 s
	II	119	Yes	350×350	200×170	2	6	0, 800	2 min 34 s
DCE	I	1.68	Yes	360×350	384×384	2	2	–	6 min 15 s
	II	2.28	Yes	360×360	288×216	4	1.6	–	5 min 21 s

TE echo time, *FOV* field of view, *T1WI* T1-weighted imaging, *T2WI* T2-weighted imaging, *DWI* diffusion-weighted imaging, *DCE* dynamic contrast-enhanced, *FS* fat suppression

Breast lesion segmentation

The whole tumor's volume-of-interest (VOI) was segmented on the peak-enhanced phase of DCE, T2WI-FS, DWI, and ADC images via ITK-SNAP software (version 3.8.0, http://www.itksnap.org) independently by two experienced radiologists in breast MRI (reader 1: Y.W.Z. from Institution I; and reader 2: Y.Q. from Institution II), independently. Readers 1 and 2 independently performed VOI segmentation on a randomly chosen subset of 50 patients from the training dataset, repeated after 2 weeks. The intra-class correlation coefficients (ICCs) of radiomics features were calculated to assess the intra-rater reproducibility (first vs. second segmentations by each reader) and inter-rater reproducibility (first segmentation by reader 1 vs. first segmentation by reader 2, second segmentation by reader 1 vs. second segmentation by reader 2) of image segmentation. ICC > 0.75 indicated satisfactory agreement.

The breast lesion segmentation was performed separately on DCE, T2WI-FS, and DWI images. For DCE, the VOIs were manually delineated on tumor-contouring slices in the peak-enhanced phase of DCE (the 2nd phase, 60 s post contrast enhancement in Institution I and the 12th phase, 96 s post contrast enhancement in Institution II), on which the tumor can be better differentiated from the neighboring tissues [18]. For DWI, the VOIs were manually drawn on DWI images (b values = 800 s/mm²). Then, VOIs of DWI were directly applied to ADC maps and manually corrected in the case of mismatched areas. During the segmentation, the VOIs were delineated to cover all the tumor areas while excluding edema, blood vessels, and normal fibroglandular tissue.

Radiomics feature extraction and selection

The radiomics analysis workflow is shown in Fig. 2. Radiomics feature extraction was conducted utilizing the Pyradiomics package (version 3.8.3, http://pyradiomics.

readthedocs.io). Before radiomics feature extraction, all segmented VOIs underwent *z*-score normalization to standardize the distribution of image voxels [19]. A total of 6432 radiomics features (1608 radiomics features each from DWI, ADC, T2WI-FS, and DCE) were obtained for each patient [20]. The extracted radiomics features included morphological features and texture features. Details of radiomics features are shown in Supplementary Table S1.

Radiomics model development and validation

Three MRI-based radiomics models were developed to differentiate (1) HER2-overexpressing *vs.* others (HER2-low-expressing + HER2-zero-expressing); (2) HER2-low-expressing *vs.* others (HER2-overexpressing + HER2-zero-expressing); and (3) HER2-zero-expressing *vs.* others (HER2-overexpressing + HER2-low-expressing). The least absolute shrinkage and selection operator (LASSO) regression method was used to select the optimal HER2 status–related radiomics features from the training dataset. The radiomics signature was represented as a radiomics score, which was computed using a formula that integrated chosen radiomics features, weighted by their corresponding coefficients obtained from LASSO regression. The predictive models were built by the selected radiomics signature in the training dataset and then tested in the independent and external validation datasets, respectively. The predictive performance of each model was quantified by the receiver operating characteristic (ROC) curve with the calculation of the area under the ROC curve (AUC).

Statistical analysis

All statistical analyses were conducted using SPSS (version 25.0; IBM Corp) and R software (version 4.1.2, https://www.r-project.org). Continuous variables were presented as means ± standard deviation, while

Zheng *et al. European Radiology* (2024) 34:6132–6144
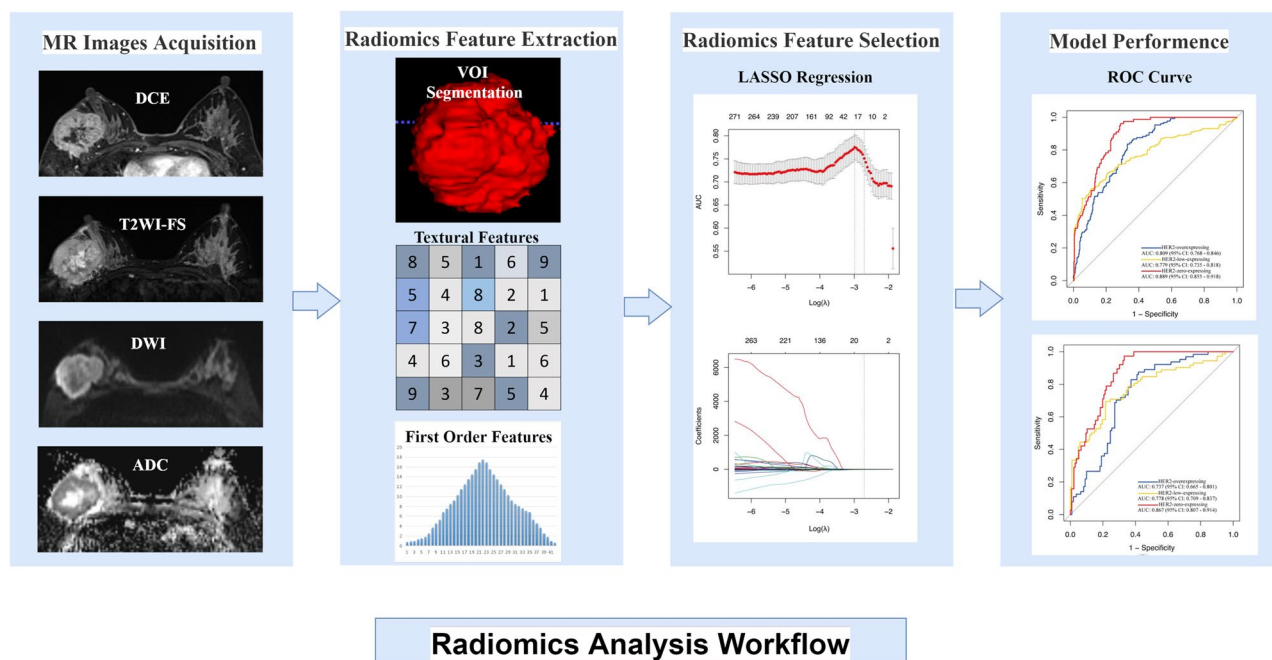
6137

Fig. 2 Workflow of radiomics analysis. Abbreviations: DCE, dynamic contrast-enhanced imaging; T2WI-FS, T2-weighted imaging fat suppression; DWI, diffusion weighted imaging; ADC, apparent diffusion coefficient; VOI, volume of interest; LASSO, shrinkage and selection shrinkage and selection operator; ROC, receiver operating characteristic

categorical variables were conveyed as absolute numbers (*n*) and their corresponding proportions (%). Differences in categorical variables among HER2-expressing statuses were evaluated with Fisher's exact or Pearson chi-square tests (i.e., family history of breast cancer, histology of breast cancer, hormone receptor status, and Ki-67 level). Differences in continuous variables among HER2-expressing statuses were evaluated with ANOVA (i.e., age and MRI-determined long diameter of breast cancer). The LASSO regression analysis was used to select the optimal HER2 status-related radiomics features and build the predictive models for discriminating different HER2 statuses. The ROC curve, along with sensitivity, specificity, and accuracy, was employed to evaluate the discriminative performance of each predictive model. $p < 0.05$ was considered statistically significant.

Results

Clinicopathologic characteristics of patients

In total, 581 patients in Institution I and 190 patients in Institution II met the inclusion criteria of our study. Patients in Institution I were randomly divided into a training dataset ($n = 407$) and an independent validation dataset ($n = 174$) with a ratio of 7:3. One hundred and ninety patients from Institution II were allocated to the external validation dataset. The clinical characteristics of patients in the training, independent validation,

and external validation datasets are shown in Table 2. Among the whole dataset, 256 (33.2%), 360 (46.7%), and 155 (20.1%) patients had HER2-overexpressing, HER2-low-expressing, and HER2-zero-expressing breast cancer, respectively. In the training dataset, 128 (31.4%), 201 (49.4%), and 78 (19.2%) patients had HER2-overexpressing, HER2-low-expressing, and HER2-zero-expressing breast cancer, respectively. In the independent validation dataset, 64 (36.8%), 72 (41.4%), and 38 (21.8%) patients had HER2-overexpressing, HER2-low-expressing, and HER2-zero-expressing breast cancer, respectively. In the external validation dataset, 64 (33.7%), 87 (45.8%), and 39 (20.5%) patients had HER2-overexpressing, HER2-low-expressing, and HER2-zero-expressing breast cancer, respectively. Hormone receptor status and Ki-67 level were significantly different among the three HER2-expressing groups in training (both $p < 0.001$), independent validation ($p < 0.001$ and $p = 0.007$, respectively), and external validation ($p = 0.001$ and $p = 0.008$, respectively) datasets. The MRI-determined long diameter of breast cancer significantly differed among the three HER2-expressing groups in the training dataset ($p < 0.001$). There were no statistically significant differences in age ($p = 0.664, 0.916, 0.084$, respectively), family history of breast cancer ($p = 0.463, 0.411, 0.165$, respectively), and histology of breast cancer ($p = 0.389, 0.715, 0.510$, respectively) among three datasets.

Table 2 Clinicopathologic characteristics of patients in training, independent validation, and external validation dataset

Clinicopathologic Characteristic	Training dataset (n=407)				Independent validation dataset (n=174)				External validation dataset (n=190)			
	HER2-over (n=128)	HER2-low (n=201)	HER2-zero (n=78)	p	HER2-over (n=64)	HER2-low (n=72)	HER2-zero (n=38)	p	HER2-over (n=64)	HER2-low (n=87)	HER2-zero (n=39)	p
Age, mean±SD (year)	50.87±10.60	50.45±10.81	51.84±11.11	0.664	51.02±10.53	51.47±10.50	51.92±11.39	0.916	48.05±9.07	51.38±10.10	48.15±11.60	0.084
Family history of breast cancer				0.463				0.411				0.165
Yes	2 (1.6)	4 (2.0)	0 (0)		0 (0)	2 (1.1)	1 (0.6)		0 (0)	3 (1.6)	0 (0)	
No	126 (31.0)	197 (48.4)	78 (19.2)		64 (36.8)	70 (40.2)	37 (21.3)		64 (33.7)	84 (44.2)	39 (20.5)	
Histology of breast cancer (%)				0.389				0.715				0.510
Invasive ductal carcinoma	111 (27.3)	174 (42.8)	72 (17.7)		58 (33.3)	63 (36.2)	35 (20.1)		55 (28.9)	79 (41.6)	36 (18.9)	
Others	17 (4.2)	27 (6.6)	6 (1.5)		6 (3.4)	9 (5.2)	3 (1.7)		9 (4.7)	8 (4.2)	3 (1.6)	
Hormone receptor status												
ER/PR − (%)	39 (9.6)	20 (4.9)	21 (5.2)	<0.001*	21 (12.1)	3 (1.7)	7 (4.0)	<0.001*	23 (12.1)	9 (4.7)	10 (5.3)	0.001*
ER/PR + (%)	89 (21.9)	181 (44.5)	57 (14.0)		43 (24.7)	69 (39.7)	31 (17.8)		41 (21.6)	78 (41.1)	29 (15.3)	
Ki-67 (%)				<0.001*				0.007*				0.008*
Low (%)	4 (1.0)	47 (11.5)	16 (3.9)		3 (1.7)	16 (9.2)	9 (5.2)		3 (1.6)	17 (8.9)	10 (5.3)	
High (%)	124 (30.5)	154 (37.8)	62 (15.2)		61 (35.1)	56 (32.2)	29 (16.7)		61 (32.1)	70 (36.8)	29 (15.3)	
MRI-determined long diameter of breast cancer, mean±SD (mm)	41.75±21.92	31.01±22.47	38.54±23.66	<0.001*	36.16±22.14	30.50±22.39	36.97±25.99	0.245	40.36±25.50	34.14±24.53	39.00±24.43	0.056

ER estrogen receptor, *PR* progesterone receptor

* p < 0.05 indicates a significant difference

Development of MRI-based radiomics models

The development and validation of the MRI-based radiomics predictive models are shown in Figs. 1 and 2. The MRI-based radiomics features associated with HER2-overexpressing, HER2-low-expressing, and HER2-zero-expressing statuses were respectively selected in the training dataset (Fig. 3). Finally, 11 radiomics features were selected for differentiating HER2-overexpressing breast cancers from others; one radiomics feature was selected for differentiating HER2-low-expressing breast cancers from others; 17 radiomics features were selected for differentiating HER2-zero-expressing breast cancers from others. The terms and corresponding coefficients of the radiomics feature in the LASSO regression model are listed in Table 3. In the training dataset, optimal MRI radiomics score cutoffs were -0.775 for HER2-overexpressing *vs.* others, 0.021 for HER2-low-expressing *vs.* others, and -1.397 for HER2-zero-expressing *vs.* others. MRI radiomics models in the training dataset achieved AUCs of 0.809 for HER2-overexpressing breast cancers *vs.* others, 0.779 for HER2-low-expressing *vs.* others, and 0.889 for HER2-zero-expressing *vs.* others, listed in Table 4.
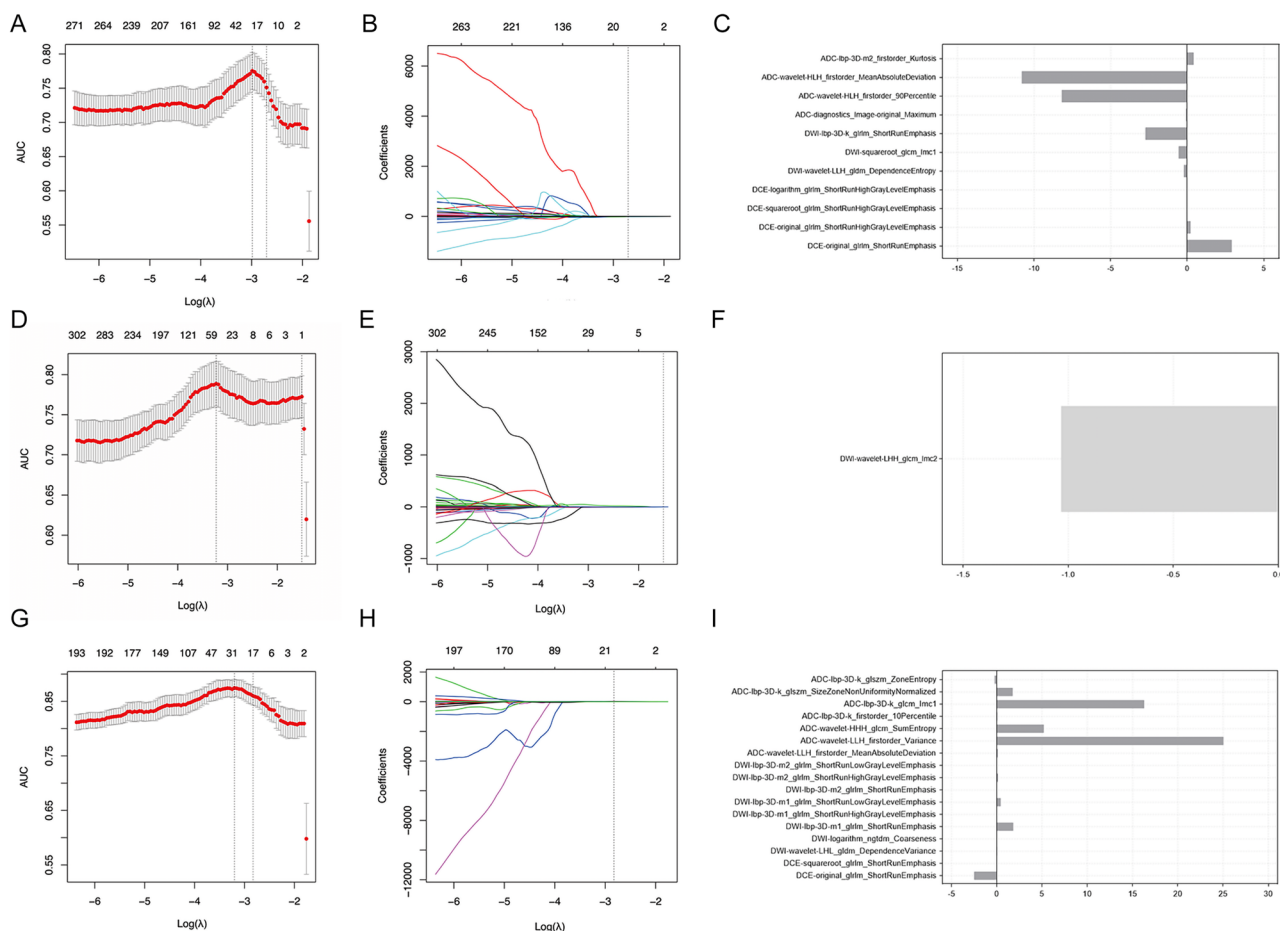
Fig. 3 Radiomics feature selection using the least absolute shrinkage and selection operator (LASSO) logistic regression. **A**, **D**, **G** The selection of tuning parameter (λ) in the LASSO model (**A** HER2-overexpressing *vs.* others; **D** HER2-low-expressing *vs.* others; **G** HER2-zero-expressing *vs.* others) using tenfold cross-validation via minimum criteria. The area under the curve (AUC) was plotted versus log (λ). A dotted vertical line was drawn at the optimal values using the minimum criteria and the one standard error of the minimum criteria. Log (λ) was set as -2.707408, -1.508029, and -2.828045, respectively, according to tenfold cross-validation in this study. **B**, **E**, **H** The dotted vertical line was plotted at the selected λ value, resulting in 11, 1, and 17 non-zero-coefficient features, respectively. **C**, **F**, **I** The correlation coefficients of the 11, 1, and 17 selected radiomics features in discriminating HER2-overexpressing status *vs.* others, HER2-low-expressing status *vs.* others, and HER2-zero-expressing status *vs.* others, respectively

Table 3 Selected radiomics features for predictive model development

Model	Radiomics Feature	Coefficient
HER2-overexpressing vs. others	Intercept	− 3.857511e-01
	DCE-original_glrlm_ShortRunEmphasis	2.905252e + 00
	DCE-original_glrlm_ShortRunHighGrayLevelEmphasis	2.183526e-01
	DCE-squareroot_glrlm_ShortRunHighGrayLevelEmphasis	3.638230e-06
	DCE-logarithm_glrlm_ShortRunHighGrayLevelEmphasis	1.265897e-15
	DWI-wavelet-LLH_gldm_DependenceEntropy	− 2.235559e-01
	DWI-squareroot_glcm_Imc1	− 5.658394e-01
	DWI-lbp-3D-k_glrlm_ShortRunEmphasis	− 2.744748e + 00
	ADC-diagnostics_Image-original_Maximum	− 8.609875e-02
	ADC-wavelet-HLH_firstorder_90Percentile	− 8.199573e + 00
	ADC-wavelet-HLH_firstorder_MeanAbsoluteDeviation	− 1.081487e + 01
	ADC-lbp-3D-m2_firstorder_Kurtosis	4.156383e-01
HER2-low-expressing vs. others	Intercept	0.4790347
	DWI-wavelet-LHH_glcm_Imc2	− 1.0341104
HER2-zero-expressing vs. others	Intercept	− 1.041099e + 01
	DCE-original_glrlm_ShortRunEmphasis	− 2.501285e + 00
	DCE-squareroot_glrlm_ShortRunEmphasis	− 4.035961e-14
	DWI-wavelet-LHL_gldm_DependenceVariance	4.055487e-02
	DWI-logarithm_ngtdm_Coarseness	6.715463e-08
	DWI-lbp-3D-m1_glrlm_ShortRunEmphasis	1.834688e + 00
	DWI-lbp-3D-m1_glrlm_ShortRunHighGrayLevelEmphasis	1.361575e-13
	DWI-lbp-3D-m1_glrlm_ShortRunLowGrayLevelEmphasis	4.440932e-01
	DWI-lbp-3D-m2_glrlm_ShortRunEmphasis	6.894049e-14
	DWI-lbp-3D-m2_glrlm_ShortRunHighGrayLevelEmphasis	1.454346e-01
	DWI-lbp-3D-m2_glrlm_ShortRunLowGrayLevelEmphasis	7.411103e-14
	ADC-wavelet-LLH_firstorder_MeanAbsoluteDeviation	1.249998e-01
	ADC-wavelet-LLH_firstorder_Variance	2.504410e + 01
	ADC-wavelet-HHH_glcm_SumEntropy	5.192917e + 00
	ADC-lbp-3D-k_firstorder_10Percentile	6.755116e-02
	ADC-lbp-3D-k_glcm_Imc1	1.628498e + 01
	ADC-lbp-3D-k_glszm_SizeZoneNonUniformityNormalized	1.757296e + 00
	ADC-lbp-3D-k_glszm_ZoneEntropy	− 2.494226e-01

DCE dynamic contrast-enhanced imaging, *DWI* diffusion-weighted imaging, *ADC* apparent diffusion coefficient

Validation of MRI-based radiomics predictive models

The predictive performance in differentiating different HER2-expressing statuses is shown in Table 4 and Fig. 4. MRI radiomics models achieved an AUC of 0.737 and 0.725 for differentiating HER2-overexpressing breast cancers from others, 0.778 and 0.782 for differentiating HER2-low-expressing breast cancers from others, and 0.867 and 0.813 for differentiating HER2-zero-expressing breast cancers from others in the independent validation and external validation datasets, respectively.

Discussion

Our study findings demonstrated that the multiparametric MRI-based radiomics predictive models had good performance in identifying HER2-overexpressing status, HER2-low-expressing status, and HER2-zero-expressing status in breast cancers with an AUC ranging from 0.725 to 0.813 in the external validation cohort. These multiparametric MRI radiomics models hold the potential to classify the HER2 status noninvasively and may assist in clinical decision-making for breast cancer.

Zheng *et al. European Radiology* (2024) 34:6132–6144

6141

Table 4 Performances of predictive models for HER2 status discrimination

| Models and datasets	AUC (95% CI)	Sensitivity (95% CI)	Specificity (95% CI)	Accuracy (95% CI)
HER2-overexpressing *vs.* others				
Training dataset	0.809 (0.768–0.846)	83.59% (76.02–89.55%)	67.03% (61.17–72.51%)	72.24% (67.61–76.53%)
Independent validation dataset	0.737 (0.665–0.801)	69.23% (56.55–80.09%)	70.00% (60.52–78.37%)	69.71% (63.71–82.52%)
External validation dataset	0.725 (0.656–0.787)	73.44% (60.91–83.70%)	62.70% (53.64–71.15%)	66.32% (62.33–76.42%)
HER2-low-expressing *vs.* others				
Training dataset	0.779 (0.735–0.818)	56.22% (49.06–63.19%)	88.35% (83.16–92.39%)	72.48% (67.87–76.77%)
Independent validation dataset	0.778 (0.709–0.837)	52.78% (40.65–64.67%)	83.33% (74.66–89.98%)	70.69% (63.33–77.33%)
External validation dataset	0.782 (0.716–0.838)	52.87% (41.87–63.67%)	88.35% (80.53–93.83%)	72.11% (65.15–78.35%)
HER2-zero-expressing *vs.* others				
Training dataset	0.889 (0.855–0.918)	96.15% (89.17–99.20%)	71.12% (65.90–75.96%)	75.92% (71.46–80.00%)
Independent validation dataset	0.867 (0.807–0.914)	89.47% (75.20–97.06%)	69.85% (61.40–77.42%)	74.14% (66.97–80.47%)
External validation dataset	0.813 (0.750–0.866)	92.31% (79.13–98.38%)	66.89% (58.77–74.32%)	72.11% (65.15–78.35%)

AUC area under the curve, *CI* confidence interval
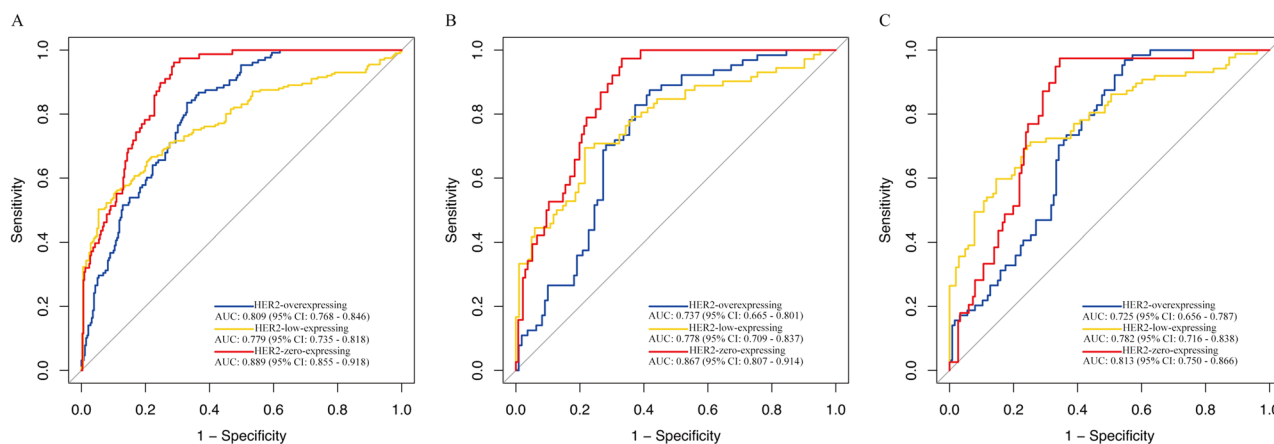
Fig. 4 Receiver operating characteristic (ROC) curves of the MRI-based radiomics predictive models for HER2 status discrimination in training (**A**), independent validation (**B**), and external validation (**C**) datasets. AUC, area under the curve; CI, confidence interval

The effectiveness of HER2-targeted therapies like trastuzumab is widely recognized in HER2-overexpressing breast cancer patients, whereas it lacks efficacy in those with HER2-negative breast cancers. However, the traditional HER2-negative breast cancer includes the population of HER2-low-expressing plus HER2-zero-expressing breast cancer, as indicated in the newly proposed classification system [21]. Previously, several single-parametric or multiparametric MRI radiomics models have been developed to differentiate HER2-overexpressing from HER2-negative breast cancers. The single-parametric MRI radiomics models showed an AUC ranging from 0.65 to 0.69 [22–24]. For example, Li et al reported an MRI radiomics model based on DCE to differentiate HER2-overexpressing from HER2-negative disease, with an AUC of 0.65 [22]. Comparatively, multiparametric MRI radiomics models showed higher performance with an AUC ranging from 0.69 to 0.887 [12–14]. For example,

Xu et al developed a multiparametric (T2WI, DCE, and ADC) MRI radiomics model incorporating a machine learning algorithm for identifying HER2-overexpressing and HER2-negative breast cancers and showed the highest AUC of 0.887 [13]. Our study developed a multiparametric MRI-based radiomics model to discriminate HER2 overexpressing breast cancers from traditionally negative HER2 status (HER2-low-expressing plus HER2-zero-expressing). The MRI radiomics model in our study incorporated radiomics features from DCE, DWI, and ADC and showed good performance with an AUC of 0.809 in the external validation dataset. The performance of our multiparametric MRI radiomics model was comparable with the previously reported multiparametric MRI radiomics models [12–14] while superior to the previously described single-parametric MRI radiomics models [23, 24]. The better performance of multiparametric MRI radiomics models may be attributed to the fact

that more complementary information can be derived from multiparametric sequences, such as morphologic findings, micro-vessel permeability, and water diffusion properties [14, 25].

Notably, the new HER2-targeted therapy approach and its clinical benefits in HER2-low-expressing breast cancer have dramatically revolutionized the clinical treatment landscape of traditional HER2-negative breast cancers [8]. A new group of patients, those with HER2-low-expressing breast cancers, is now recognized as having potential benefits from novel HER2-targeted therapies. The clinicopathologic characteristics and targeted therapies of this new group of breast cancer have been elucidated [2–4, 26, 27]. A combined assessment of patients from four clinical trials revealed notable distinctions between HER2-low-expressing breast cancers and HER2-zero-expressing breast cancers in biologic features, clinicopathologic findings, therapeutic response, and clinical outcome [2]. A recent phase III clinical trial showed that trastuzumab deruxtecan (a kind of antibody–drug conjugate) significantly improved the survival time in individuals with advanced HER2-low-expressing breast cancer compared with the chemotherapy, highlighting the clinical significance of the HER2-low-expressing, and the need to redefine this subgroup from the traditional HER2-negative breast cancers [3].

Recently, two studies indicated the potential utility of MRI-based radiomics models for predicting HER2 status, including the HER2-low-expressing category [15, 16]. Ramtohul et al reported that the MRI-based radiomics signature achieved an AUC ranging from 0.78 to 0.79 for discriminating HER2-low plus HER2-over *vs.* HER2-zero breast cancers [15]. The established MRI-based radiomics signature involved 6 radiomic features from T2WI and one radiomic feature from T1 contrast-enhanced images [15]. Further, they built a combined model incorporating the pathologic feature (i.e., histology type) and MRI findings (i.e., nonmass enhancement and multiple lesions) for the prediction of HER2-low *vs.* HER2-positive cancers, with a reported AUC of 0.78 and 0.77 in the training and external dataset, respectively [15]. Bian et al reported that two MRI radiomics signatures were able to distinguish HER2-overexpressing from HER2-negative (AUCs range, 0.760 to 0.793) and HER2-low from HER2-negative breast cancers (AUCs range, 0.711 to 0.820) [16]. One radiomics signature consisting of 13 radiomic features (6 features from T1-weighted contrast-enhanced images and 7 features from ADC images) was found to be able to distinguish HER2-overexpressing *vs.* HER2-negative cancers. Another radiomics signature consisting of 9 radiomics features (6 features from T1-weighted contrast-enhanced images and 3 features from ADC images) was developed to differentiate the

HER2-low *vs.* HER2-negative cancers [16]. In our study, we extracted high-throughput radiomics features from four imaging sequences to construct MRI radiomics models to differentiate the newly proposed HER2 expression statutes of breast cancer. A total of 6432 radiomics features (1608 radiomics features each from DWI, ADC, T2WI-FS, and DCE) were extracted from each patient. Then, we developed and validated MRI-based radiomics models to differentiate each HER2-expressing status (i.e., HER2-overexpressing status, HER2-low-expressing status, and HER2-zero-expressing) from other statuses. Our study showed that the predictive model with 11 radiomics features, including 3 features from DWI, 4 from ADC, and 4 from DCE images, had AUCs ranging from 0.725 to 0.809 in differentiating HER2 overexpressing breast cancers from HER2-low-expressing plus HER2-zero-expressing breast cancers. In addition, a predictive model with one radiomics feature from DWI had AUCs ranging from 0.778 to 0.782 in differentiating HER2-low-expressing breast cancers from HER2-overexpressing plus HER2-zero-expressing breast cancers. Finally, a predictive model with 17 radiomics features, including 2 features from DCE, 8 from DWI, and 7 from ADC images, was developed and validated to differentiate HER2-zero-expressing from HER2-overexpressing plus HER2-low-expressing breast cancers with AUCs ranging from 0.813 to 0.889. However, no radiomics feature from T2WI was selected to develop the radiomics model, which may indicate that the radiomics features derived from DWI, ADC, and DCE have stronger capability for discriminating different HER2-expressing statuses. These results showed that features derived from multiparametric (i.e., DWI, ADC, and DCE) MRI radiomics hold the potential as a noninvasive tool for identifying the HER2-overexpressing, HER2-low-expressing, and HER2-zero-expressing breast cancers, which might help to determine potential candidates for traditional anti-HER2 therapy, new anti-HER2 antibody–drug conjugates therapy, or patients who may be excluded from anti-HER2 treatment.

There were some limitations in our study. First, since the study was conducted retrospectively, potential bias in patient selection may exist. Second, to compute the ROC curve for a three-classification event, we changed the three-classification to two-classification to distinguish different HER2-expressing statuses. More advanced statistical methods might solve this drawback. Third, the tumor VOI segmentation was performed manually, and the traditional handcrafted radiomics feature extraction was time-consuming and complicated. These might be overcome with a more automatic segmentation approach, such as deep learning frameworks.

In summary, our study demonstrated that multiparametric MRI-based radiomics models hold potential as

Zheng *et al. European Radiology* (2024) 34:6132–6144

6143

a noninvasive tool to discriminate the HER2-expressing status in breast cancer patients. Pretreatment identification of HER2-low-expressing from other kinds of HER2-expressing breast cancers will facilitate the refinement of anti-HER2 therapy in breast cancer patients.

Abbreviations

ADC	Apparent diffusion coefficient
AUC	Area under the curve
DCE	Dynamic contrast-enhanced
DWI	Diffusion-weighted imaging
ER	Estrogen receptor
FS	Fat suppression
HER-2	Human epidermal growth factor receptor-2
ICC	Intra-class correlation coefficient
IHC	Immunohistochemistry
ISH	In situ hybridization
LASSO	Least absolute shrinkage and selection operator
PR	Progesterone receptor
ROC	Receiver operating characteristic
T1WI	T1-weighted imaging
T2WI	T2-weighted imaging
VOI	Volume of interest

Supplementary Information

The online version contains supplementary material available at https://doi.org/10.1007/s00330-024-10641-7.

> Below is the link to the electronic supplementary material. Supplementary file1 (PDF 303 KB)

Declarations

Guarantor

The scientific guarantor of this publication is Xiang Zhang.

Conflict of interest

The authors of this manuscript declare no relationships with any companies, whose products or services may be related to the subject matter of the article.

Statistics and biometry

One author (Zehong Yang) has statistical expertise.

Informed consent

Written informed consent was waived by the Institutional Review Board.

Ethical approval

Institutional Review Board approval was obtained from the Institutional Review Board of Shantou Central Hospital (Shantou, China) ([2022] Research 072), Sun Yat-Sen Memorial Hospital, Sun Yat-Sen University (Guangzhou, China) (SYSKY-2023–788-01).

Study subjects or cohorts overlap

No study subject or cohort has been previously reported in this study.

Methodology

- retrospective
- diagnostic study
- multicenter study

Author details

[1]Department of Radiology, Shantou Central Hospital, No. 114 Waima Road, Shantou 515031, People's Republic of China. [2]Department of Radiology, Sun Yat-Sen Memorial Hospital, Sun Yat-Sen University, No. 107 Yanjiang Road West, Guangzhou 510120, People's Republic of China. [3]Guangdong Provincial Key Laboratory of Malignant Tumor Epigenetics and Gene Regulation, Medical Research Center, Sun Yat-Sen Memorial Hospital, Sun Yat-Sen University, No. 107 Yanjiang Road West, Guangzhou 510120, People's Republic of China.

References

1. Siegel RL, Miller KD, Fuchs HE, Jemal A (2022) Cancer statistics, 2022. CA Cancer J Clin 72:7–33
2. Denkert C, Seither F, Schneeweiss A et al (2021) Clinical and molecular characteristics of HER2-low-positive breast cancer: pooled analysis of individual patient data from four prospective, neoadjuvant clinical trials. Lancet Oncol 22:1151–1161
3. Modi S, Jacot W, Yamashita T et al (2022) Trastuzumab deruxtecan in previously treated HER2-low advanced breast cancer. N Engl J Med 387:9–20
4. Tarantino P, Hamilton E, Tolaney SM et al (2020) HER2-low breast cancer: pathological and clinical landscape. J Clin Oncol 38:1951–1962
5. Miglietta F, Griguolo G, Bottosso M et al (2021) Evolution of HER2-low expression from primary to recurrent breast cancer. NPJ Breast Cancer 7:137
6. Fan P, Xu K (2023) Antibody-drug conjugates in breast cancer: marching from HER2-overexpression into HER2-low. Biochim Biophys Acta Rev Cancer 1878:188849
7. Miglietta F, Griguolo G, Bottosso M et al (2022) HER2-low-positive breast cancer: evolution from primary tumor to residual disease after neoadjuvant treatment. NPJ Breast Cancer 8:66
8. Prat A, Bardia A, Curigliano G et al (2022) An overview of clinical development of agents for metastatic or advanced breast cancer without ERBB2 amplification (HER2-low). JAMA Oncol https://doi.org/10.1001/jamaoncol.2022.4175
9. Loibl S, Gianni L (2017) HER2-positive breast cancer. Lancet 389:2415–2429
10. Bitencourt AGV, Gibbs P, Rossi Saccarelli C et al (2020) MRI-based machine learning radiomics can predict HER2 expression level and pathologic response after neoadjuvant therapy in HER2 overexpressing breast cancer. EBioMedicine 61:103042
11. Kazerouni AS, Hormuth DA 2nd, Davis T et al (2022) Quantifying tumor heterogeneity via MRI habitats to characterize microenvironmental alterations in HER2+ breast cancer. Cancers (Basel) 14:1837
12. Fang C, Zhang J, Li J et al (2022) Clinical-radiomics nomogram for identifying HER2 status in patients with breast cancer: a multicenter study. Front Oncol 12:922185
13. Xu A, Chu X, Zhang S et al (2022) Development and validation of a clinicoradiomic nomogram to assess the HER2 status of patients with invasive ductal carcinoma. BMC Cancer 22:872
14. Zhou J, Tan H, Li W et al (2021) Radiomics signatures based on multiparametric MRI for the preoperative prediction of the HER2 status of patients with breast cancer. Acad Radiol 28:1352–1360
15. Ramtohul T, Djerroudi L, Lissavalid E et al (2023) Multiparametric MRI and radiomics for the prediction of HER2-zero, -low, and -positive breast cancers. Radiology 308:e222646
16. Bian X, Du S, Yue Z et al (2023) Potential antihuman epidermal growth factor receptor 2 target therapy beneficiaries: the role of MRI-based

6144

Zheng *et al. European Radiology* (2024) 34:6132–6144

radiomics in distinguishing human epidermal growth factor receptor 2-low status of breast cancer. J Magn Reson Imaging 58:1603–1614

17. Wolff AC, Hammond MEH, Allison KH et al (2018) Human epidermal growth factor receptor 2 testing in breast cancer: American Society of Clinical Oncology/College of American Pathologists Clinical Practice Guideline Focused Update. Arch Pathol Lab Med 142:1364–1382

18. Peng S, Chen L, Tao J et al (2021) Radiomics analysis of multi-phase DCE-MRI in predicting tumor response to neoadjuvant therapy in breast cancer. Diagnostics (Basel) 11:2086

19. Ellingson BM, Zaw T, Cloughesy TF et al (2012) Comparison between intensity normalization techniques for dynamic susceptibility contrast (DSC)-MRI estimates of cerebral blood volume (CBV) in human gliomas. J Magn Reson Imaging 35:1472–1477

20. van Griethuysen JJM, Fedorov A, Parmar C et al (2017) Computational radiomics system to decode the radiographic phenotype. Cancer Res 77:e104–e107

21. Tarantino P, Viale G, Press MF et al (2023) ESMO expert consensus statements (ECS) on the definition, diagnosis, and management of HER2-low breast cancer. Ann Oncol 34:645–659

22. Li H, Zhu Y, Burnside ES et al (2016) Quantitative MRI radiomics in the prediction of molecular classifications of breast cancer subtypes in the TCGA/TCIA data set. NPJ Breast Cancer 2:16012

23. Li C, Song L, Yin J (2021) Intratumoral and peritumoral radiomics based on functional parametric maps from breast DCE-MRI for prediction of HER-2 and Ki-67 status. J Magn Reson Imaging 54:703–714

24. Song L, Li C, Yin J (2021) Texture analysis using semiquantitative kinetic parameter maps from DCE-MRI: preoperative prediction of HER2 status in breast cancer. Front Oncol 11:675160

25. Liu Z, Li Z, Qu J et al (2019) Radiomics of multiparametric MRI for pretreatment prediction of pathologic complete response to neoadjuvant chemotherapy in breast cancer: a multicenter study. Clin Cancer Res 25:3538–3547

26. Takegawa N, Tsurutani J, Kawakami H et al (2019) [fam-] trastuzumab deruxtecan, antitumor activity is dependent on HER2 expression level rather than on HER2 amplification. Int J Cancer 145:3414–3424

27. Zhang H, Peng Y (2022) Current biological, pathological and clinical landscape of HER2-low breast cancer. Cancers (Basel) 15:126

Publisher's Note